

**Evaluating the Static Segregation Resistance of Hardened Self-Consolidating Concrete
using Image Processing Technology**

Chuanxin Fang, Ph.D. P.E. (Corresponding Author)

Senior Engineer
Applied Research Associates, Inc.
505 West University Avenue
Champaign, IL 61821
Ph: (217) 356-4500
Fax: (217) 356-2088
Email: ffang@ara.com

Samuel Labi

School of Civil and Environmental Engineering/CTPID
Massachusetts Institute of Technology
77 Massachusetts Avenue, E1-175
Cambridge, MA 02139
Ph: (617) 253-9725
Fax: (617) 258-8168
Email: labi@mit.edu

Submission Date: August 6, 2006
Number of Words in Text: 3,945
Number of Tables: 5
Number of Figures: 9
Total Equivalent Number of Words: 7,445

For Presentation at the 86th Annual Meeting of the Transportation Research Board.

ABSTRACT

Self-consolidating concrete (SCC) is a highly flowable, non-segregating concrete that spreads into place, fills formwork, and encapsulates reinforcement without mechanical consolidation. SCC is increasingly being used worldwide because it has been found to offer a high-quality product with significant reductions in equipment use, construction time, labor, and construction noise. The stability, or static segregation resistance, of this new concrete type is typically assessed in terms of a Hardened Visual Stability Index (HVSI). Traditionally, HVSI assessment is based on visual judgment and is therefore severely limited by human error, low efficiency, and work tedium. As such, the present study developed and implemented a methodology for automatically evaluating SCC stability. This was done in several steps: first, converting the image of a typical concrete sample (a cut surface with various shades of grey) into a binary image of light colors (aggregates) and dark colors (concrete cement), identifying aggregate sizes, detecting the mortar layer thickness, and finally, using statistical analysis to derive the HVSI. Algorithms were developed for each phase and were implemented using standard coding languages. In effect, the methodology digitally processes a given concrete sample image and assesses its stability in terms of HVSI. The accuracy of the new methodology was checked using control observations and was found to provide a reliable assessment of SCC stability in terms of static segregation resistance.

INTRODUCTION

Self-consolidating concrete (SCC) is an innovative, non-segregating concrete that does not require mechanical consolidation (vibration) for placing and compaction. SCC is able to flow under its own weight, completely filling formwork and achieving full compaction even in the presence of congested reinforcement. The hardened concrete is dense, homogeneous and has the same engineering properties and durability as traditional vibrated concrete (1,2). Since the 1980s when SCC was first introduced in Europe and Japan, there has been worldwide application of this concrete type for precast, prestressed, or cast-in-place concrete construction. The benefits of SCC include quick concrete placement, faster construction times and enhanced flow around congested reinforcement. The fluidity and segregation resistance of SCC helps to achieve a high degree of mix homogeneity, minimal concrete voids and uniform concrete strength, and provides the potential for a superior level of finish and durability to the structure (3). SCC is often produced with low water-cement ratio and provides the potential for early attainment of specified strengths, earlier demolding, and consequently, quicker opening of the facility to public use (2). The elimination of mechanical consolidation equipment leads to savings in equipment use and labor, improved environmental quality in the construction area, and reduced exposure of construction workers and surrounding areas to equipment noise and vibration. With such improvements in construction delivery, worker health/safety and environmental impacts, SCC has become an increasingly attractive option for concrete construction.

A major issue associated with SCC, however, is that it has two plastic state properties: *flowability* (ability to flow into and within intended enclosure) and *stability* or *static segregation resistance* (the ability to withstand undue separation of aggregate and sand-cement). Flowability is generally attained using high-range, water-reducing admixtures; stability is attained using a certain specified aggregate gradation pattern and/or by using admixtures that modify concrete viscosity (4).

Agencies are developing and/or implementing several new test methods to characterize the properties of SCC. Flowability, for example, is measured in terms of the spread of the fresh concrete sample using a modified version of the slump test (5). The J-Ring, U-Box, and AL-Box tests measure the passing ability of concrete in congested reinforcement (6). At the Illinois Department of Transportation (IDOT), SCC stability is assessed visually, using protocols described in the Illinois Test Procedure SCC-6 – Test Method for Static Segregation of Hardened Self-Consolidating Concrete Cylinders (7). This test, which has been used since 2003, involves casting or coring concrete, cutting the core lengthwise in two, visually examining the extent of segregation, and expressing such stability in terms of a Hardened Visual Stability Index (HVSI). HVSI ratings have four levels that are based on the length of top concrete mortar layer and variance in size and coverage of coarse aggregate distribution from top to bottom of concrete sample. Illustrations of HVSI ratings for cut concrete surface images are provided in FIGURE 1.

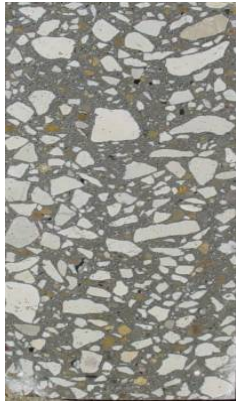



Rating	0 (Stable)	1 (Stable)	2 (Unstable)	3 (Unstable)
Image				
Description	No mortar layer at the top of the cut plane and no variance in size and percent area of coarse aggregate distribution from top to bottom.	No mortar layer at the top of the cut plane but slight variance in size and percent area of coarse aggregate distribution from top to bottom.	Slight mortar layer, less than 25 mm (1 in.) tall, at the top of the cut plane and distinct variance in size and percent area of coarse aggregate distribution from top to bottom.	Clearly segregated as evidenced by a mortar layer greater than 25 mm (1 in.) tall and/or considerable variance in size and percent area of coarse aggregate distribution from top to bottom.

FIGURE 1 Rating Criteria for Hardened Specimen Visual Stability Index (HVSI).

While the traditional (visual) assessment of HVSI has been proven to be fairly effective in measuring SCC stability, it faces several limitations such as lack of adequate experienced HVSI raters, errors in human judgment, subjectivity of the ratings, and tediousness and low efficiency of the test process, particularly when there are a large number of concrete samples.

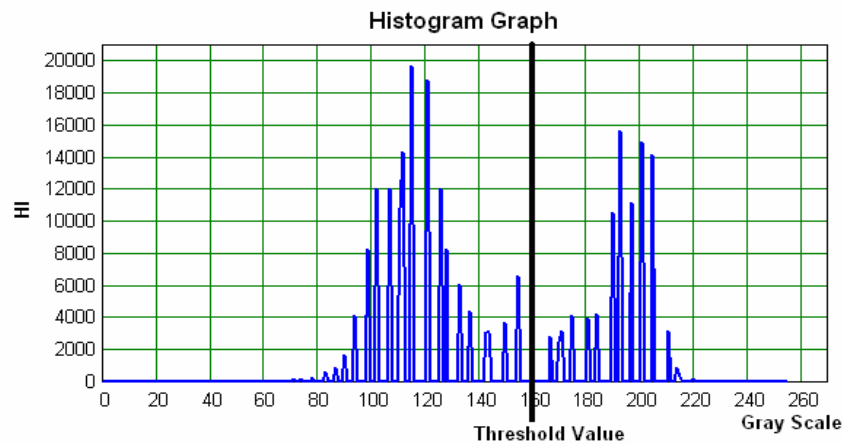
The object of this study is to develop a quick, consistent, and reliable automated system for measuring SCC stability by digitally processing the image of the cut concrete surface. This paper describes a study effort that set out to realize this objective using image processing technology. Specifically, the steps of the study, as reflected in this organization of this paper, are as follows:

- Segmentation of the cut concrete image as a binary image that identifies and separates relatively light areas and relatively grey areas, and detecting the sizes and positions of all identified aggregates.
- Detection of the mortar layer (the position where there is a sudden significant change in aggregate coverage) by scanning the image from top to bottom.
- Statistical analyses for aggregate areas and measuring the degree of variance in size and aggregate coverage.
- Determining the HVSI on the basis of the measured variance and the detected length of the mortar layer.

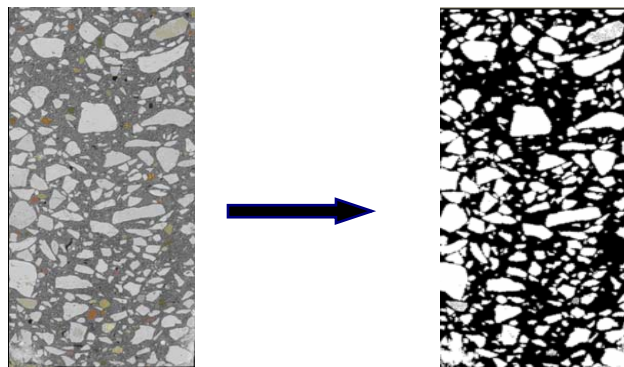
The paper describes each of the above steps and presents analytical methods, sample SCC images and their HVSI rating results, and validation of the test results.

AGGREGATE DETECTION

In a grey-level image of a cut concrete surface of a test cylinder, the color of aggregates tends to be light grey while that of concrete cement tends to be dark grey and is fairly uniform. The first step of aggregate detection, therefore, was to use this dichotomy of concrete color to segment the grey image to yield a binary image in which aggregates appear as white objects and concrete cement appears as the black background. The bifurcation of the cut concrete surface color greatly simplified the image processing procedure and time, and it was methodologically achieved by establishing a histogram of grey color intensity levels in the image, and then thresholding the image at a particular intensity level by analyzing the histogram (8). A thresholding procedure from a freely available image processing library (9) was used to convert the grey-level image into a binary (black and white) image. Illustrating the concept of grey image binary segmentation, FIGURE 2 (a) shows the histogram of the image and the optimized threshold value at 160. FIGURE 2 (b) shows the gray image and the binary image which was segmented based on the threshold value. During the color segmentation in this example, any pixel scales below the threshold value (160) were converted black, while any pixel scales above the threshold value converted as white.



a) Image Histogram and Threshold Value



b) Original and Binary Images

FIGURE 2 Grey Image Binary Segmentation.

The next step was to recognize the aggregate positions as a prelude to the subsequent determination of the size and location of the aggregate.

Aggregate Recognition

Using the binary image established at the aggregate detection step, aggregates were then recognized by collecting each white pixel and assembling (and linking) all connected pixels that are perceived to constitute an individual aggregate. A labeled link-list (10) served as the data structure used for the algorithm for this task. Two white pixels are defined as “connected” if they are only vertically or horizontally adjacent – pixels that are only diagonally adjacent are not considered connected. Therefore, at a given pixel position during scanning, the connection to other pixels only needs to be checked with two positions, the top and left pixels. This is because the order of pixel scanning is as follows: rows are scanned from top to bottom; and in each row, scanning proceeds from left to right. The connection with the right and bottom pixels is checked at a later stage when the scanning process reaches those pixels. TABLE 1 illustrates each step of aggregate recognition that uses four operations on a given white pixel “A” based on the colors of top and left adjacent pixels, “B” and “C”. TABLE 2 illustrates the aggregate recognition procedure for an image that is five pixels long and five pixels wide. This algorithm involves several link-list operations, but the image needs to be scanned only once so that each aggregate in the image can be labeled on the link-list. Any additional information required for identifying the aggregate can simply be obtained from the labeled link-lists rather than reprocessing the image. At the end of the scanning process, all white pixels found to be connected are assembled to constitute a single aggregate.

TABLE 1 Aggregate Recognition Operation

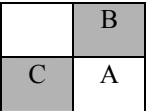
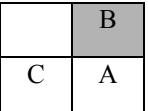
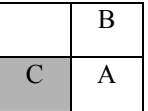
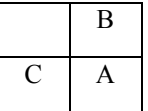
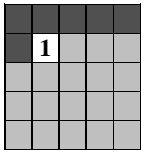
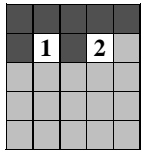
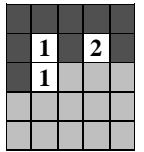
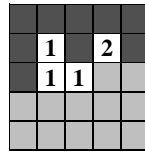
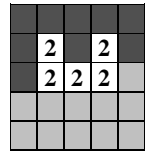


Case Number	Case I	Case II	Case III	Case IV
General Pixel Positions	 B, C are black	 B is black, C is white	 B is white, C is black	 B, C are white
Operation	Create a new label link for A	Add A into the link for C	Add A into the link for B	Add A into the link for B, and merge Links for B and for C

TABLE 2 Illustration of the Pixel Collection Operation

Position	(2,2)	(2,4)	(3,2)	(3,3)	(3,4)	(5,2)	(5,5)
Operation	Case I	Case I	Case III	Case II	Case IV	Case I	N/A
Pixels							

Aggregate Area and Size

Aggregate recognition is followed by determination of aggregate areas and sizes. The area occupied by each aggregate can be simply computed as the product of the unit pixel area and the total number of pixels on its link-list. The unit pixel area can be determined from the known concrete cylinder dimension and the image dimension in terms of the number of pixels. It is assumed that each aggregate occupies a shape that is roughly circular and that the aggregate size is represented by the diameter of that area.

MORTAR LAYER DETECTION

Heavy coarse aggregate tends to settle to the bottom of fresh concrete while mortar (with little or no coarse aggregate) tends to remain at the top (FIGURE 3). This process, known as *segregation* of the coarse aggregate from mortar, is particularly experienced in concrete of high flowability. Segregation therefore yields two layers: an upper *mortar layer* and a lower *remaining layer*. The depth of the mortar layer is an indication of the extent of concrete segregation and is therefore an important criterion in the evaluation of the HVSI index. By facilitating the determination of mortar layer depth, image processing technology helps determine the extent of concrete segregation. The procedure for detecting the length of mortar layer includes an estimation of the average aggregate area in the remaining layer. Scanning proceeds from top to bottom of the concrete sample image, and at any point of the scanning process, the average area occupied by aggregates is computed. As the scanning proceeds, any significant increase in the average aggregate area is flagged as the “transition” or “boundary” zone between the upper mortar layer and the lower remaining layer. With this knowledge of the initial scanning location and the transition line, the depth of the mortar layer can then be measured.

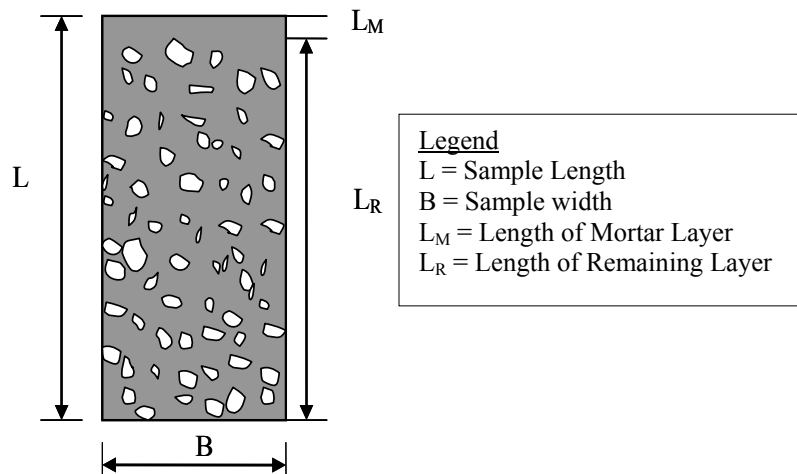
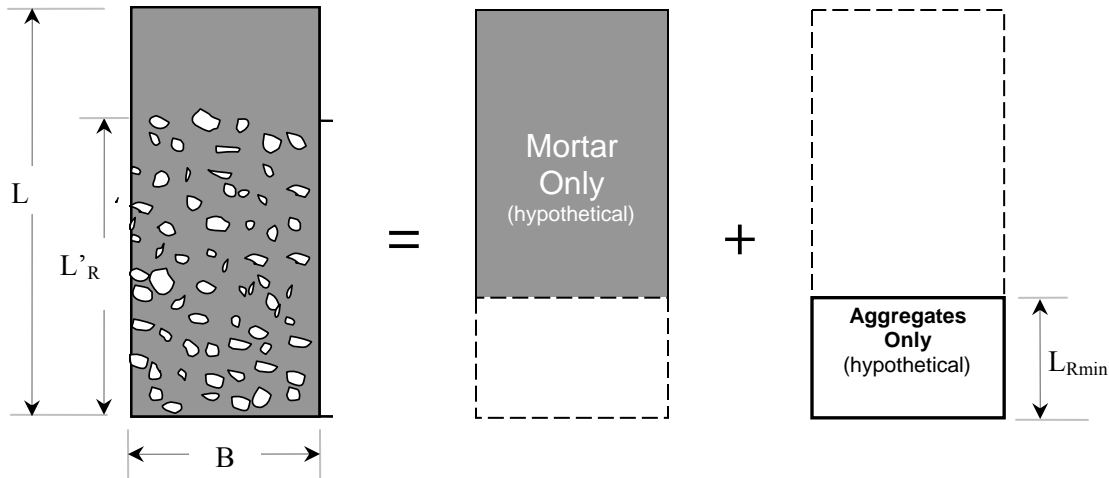


FIGURE 3 Lengths of Mortar and Remaining Layers.

Estimating the Average Aggregate Area

In this step, the minimum length of remaining layer was first calculated. Then the average aggregate area along the minimum length of the remaining layer was calculated and used to represent the average aggregate area in the total length of the remaining layer (FIGURE 4).

As can be inferred from FIGURE 4, the greater the segregation, the smaller the length of the remaining layer. Therefore, the minimum length of the remaining layer is the worst (hypothetical) segregation scenario where all (and only) aggregates bunch together as a solid mass at the bottom of the sample.



Legend

L = Sample Length, B = Sample width, L_{Rmin} = Minimum Length of Remaining Layer
 L'_R = Length of Remaining Layer

FIGURE 4 Minimum Length of Remaining Layer.

The total aggregate area, therefore, is the product of the minimum length of the remaining layer, L_{Rmin} and the sample width, B . Therefore, L_{Rmin} is calculated as:

$$L_{Rmin} = \frac{\sum A_i}{B} \quad (i=0,1,2,\dots,L)$$

where $\sum A_i$ ($i = 0,1,2,\dots,L$) is the sum of aggregate areas in each incremental horizontal strip from the top (length = 0) to the bottom (length = L).

The average of aggregate area (A_{avg}) of the sample per incremental horizontal strip along the length of the remaining layer can therefore be obtained as:

$$A_{avg} = \frac{\sum A_i}{L_{Rmin}} \quad (i=L-L_{Rmin},\dots,L)$$

Since L_{Rmin} is the minimum length of the remaining layer, A_{avg} is calculated only for the lower part of remaining layer (excluding the mortar layer) denoted by L'_R in FIGURE 4. It is therefore reasonable to represent the average of aggregate area in the total remaining layer by A_{avg} , so that:

$$L'_R \approx \frac{\sum A_i}{A_{avg}} \quad (i=L-L'_R,\dots,L)$$

where, L'_R is estimated length of the remaining layer (as shown in FIGURE 4). Since the fraction of the aggregate area in the mortar layer is relatively negligible, $\sum A_i$ ($i = L - L'_R, \dots, L$) is close to $\sum A_i$ ($i = 0, \dots, L$). The length of remaining layer can be estimated as follows:

$$L'_R \approx \frac{\sum A_i}{A_{avg}} \quad (i = 0, \dots, L).$$

Therefore, the average of aggregate areas in the remainder layer A'_{avg} can be estimated as follows:

$$A'_{avg} = \frac{\sum A_i}{L'_R} \quad (i = L - L'_R, \dots, L).$$

The estimated length of the remaining layer (L'_R) and average of aggregate areas (A'_{avg}) are used to determine the final mortar layer in the following section. The estimated length of remaining layer exceeds that of the minimum length of remaining layer, and there are more aggregate used in the estimation of average aggregate area. As such, in order to increase the estimation reliability, A'_{avg} instead of A_{avg} is used as the estimated average of aggregate areas.

Determining the Length of Mortar Layer

FIGURE 5 illustrates how the length of the mortar layer is determined. This is done on the basis of the relationship between the aggregate area and image length. The x-axis represents the image length in the top-to-bottom direction, and the y-axis represents the aggregate area at each length unit (mm). To identify the mortar layer, the image is first scanned top-to-bottom to identify the position P_M where the aggregate area first reaches the estimated aggregate coverage (A'_R). Then starting from the position P_M , the image is scanned in the reverse direction to determine the position, P'_M where the aggregate area is same as the average of aggregate area in the current mortar layer (A'_M). Lastly, if the estimated value of A'_M is significantly less than the A'_R , the position P'_M is considered as the transition boundary between the mortar layer and the remaining layer. The first two steps are to identify the sudden change of the aggregate areas along the image length, and the last step is to determine whether the top section of detection satisfies the detection criteria established for the mortar layer.

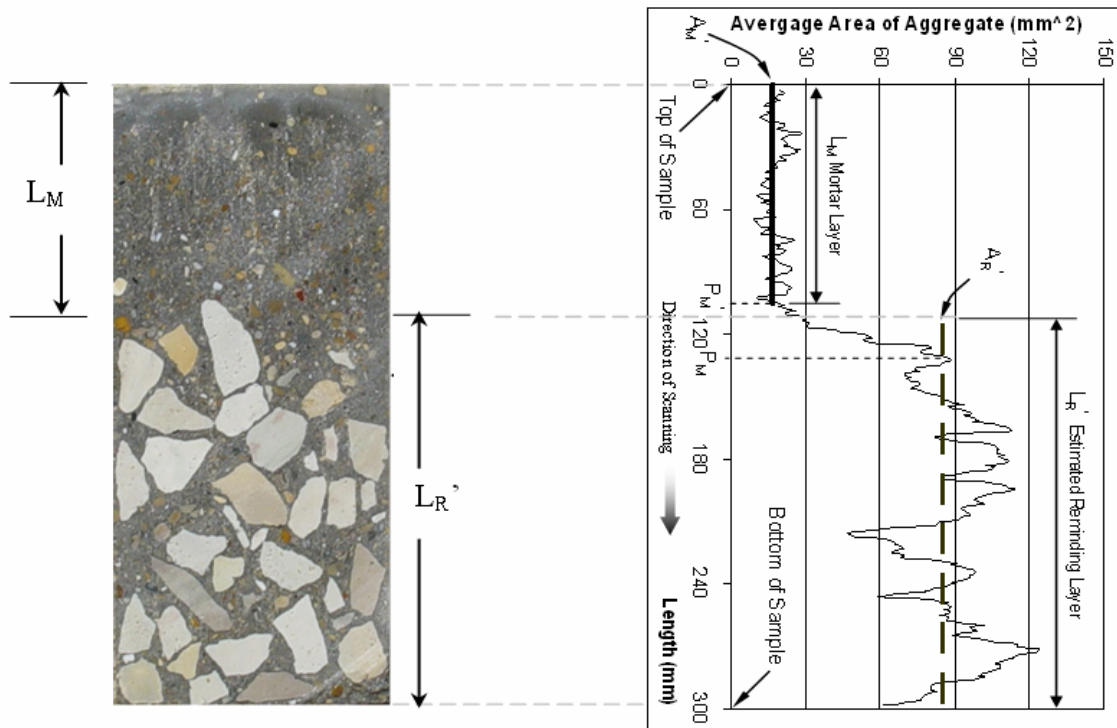


FIGURE 5 Determination of the Length of the Mortar Layer – Example.

In the actual concrete cylinder sample shown as FIGURE 5, the estimated position length of the remaining layer starts at a depth of 115mm from the top of the sample and ends at the bottom of the sample (depth of 300mm from the top). The length of the remaining layer is, therefore, 185mm. The average of aggregate areas is approximately 85 mm^2 . At the first step, the position at length 135 mm is identified as P_M where the aggregate area is equal to A_R' . At the second step, the position at length 105 mm is identified as P_M' where the aggregate area is equal to A_M' . Since A_M' is significantly less than A_R' , the position P_M' at the length 105mm is determined as the boundary position.

EVALUATING THE AGGREGATE SIZE DISTRIBUTION

By statistically analyzing the averages of aggregate areas at each 5mm-length segment in the remaining layer, the distribution of aggregate areas all along the sample length can be determined. This is done on the basis of the variance in aggregate size and also in aggregate coverage from the top to bottom. Variance was calculated for each of three sections of the remaining layer (shown in FIGURE 6) and also for three aggregate size ranges. The variance in aggregate size in each aggregate size range between each pair of top (Section 1), middle (Section 2) and bottom (Section 3) sections were computed. This was done using studentized t tests. Since the larger aggregates have a greater impact on the final evaluation of aggregate variance, different variance weights were given on the basis of their statistical P-values and aggregate size (TABLE 3). The sum of the variance indices gives the variance weight (TABLE 3) and the minimum and maximum *variance weights* are 0 to 42, respectively. The variance classification depends on the variance weight (0 – 15 is Low; 16 – 23 is Medium; and 24 – 42 is High). The boundary is initially set at 15 and 23 is to guarantee the image is rated as Medium if there are two strongly significant test results (P-Value > 0.025) in aggregate size range III, and is rated as the High if there are three strongly significant test results in aggregate size range III.

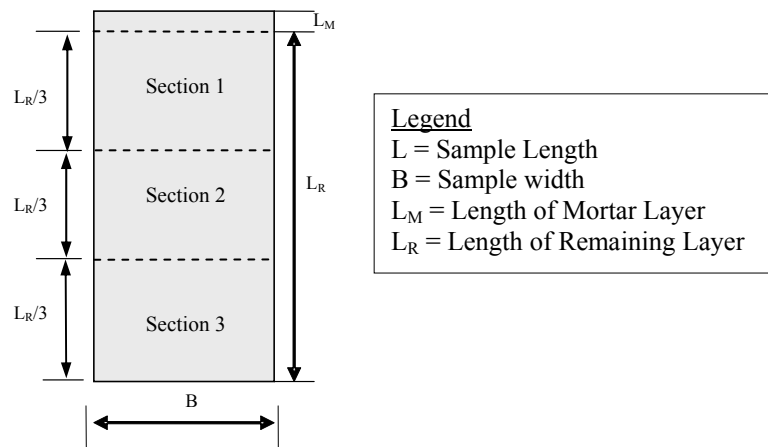


FIGURE 6 Lengths of Mortar and Remaining Layers.

TABLE 3 Criteria for Assigning Aggregate Size Variance Indices and Weights

Section Comparison	Aggregate Size Range	P-Value	Variance Index
Section 1 V.S. Section 2	Range I (Small) From 4.75 to 9.5 mm	> 0.05	0
		0.05 to 0.025	1
		≤ 0.025	2
Section 2 V.S. Section 3	Range II (Medium) From 9.6 to 16.0 mm	> 0.05	0
		0.05 to 0.025	2
		≤ 0.025	4
Section 3 V.S. Section 1	Range III (Large) From 16.1 to 50.0 mm	> 0.05	0
		0.05 to 0.025	4
		≤ 0.025	8
Sum of Variance Indices = Variance weight =			0 – 42

Note: Variance classification level is a function of the total value of indexes is as follows:
Total Variance: Low: 0 – 15; Medium: 16 – 23; High: 24 – 42.

Computer algorithms were written for the three processes of aggregate detection (aggregate recognition, aggregate area and size determination, boundary tracking), mortar layer detection (estimating the average aggregate area and determining the length of the mortar layer) and evaluating the aggregate size distribution.

Implementation of the Algorithms

The algorithms developed for each step of the concrete stability assessment methodology were implemented in computer language with a user-friendly Visual C++ interface. In the screenshot (FIGURE 7), the interface comprises three sections, an Image Viewer, a Tool Viewer, and a Graphic Viewer. The Image Viewer displays both the original image and processed image of the concrete cylinder sample. The Tool Viewer allows users to input cylinder size, and to change image processing criteria such as aggregate size range and image color levels. The graphic view displays the image histogram, digitized aggregate sizes and positions, mortar layer detection, and summary table for statistical analyses.

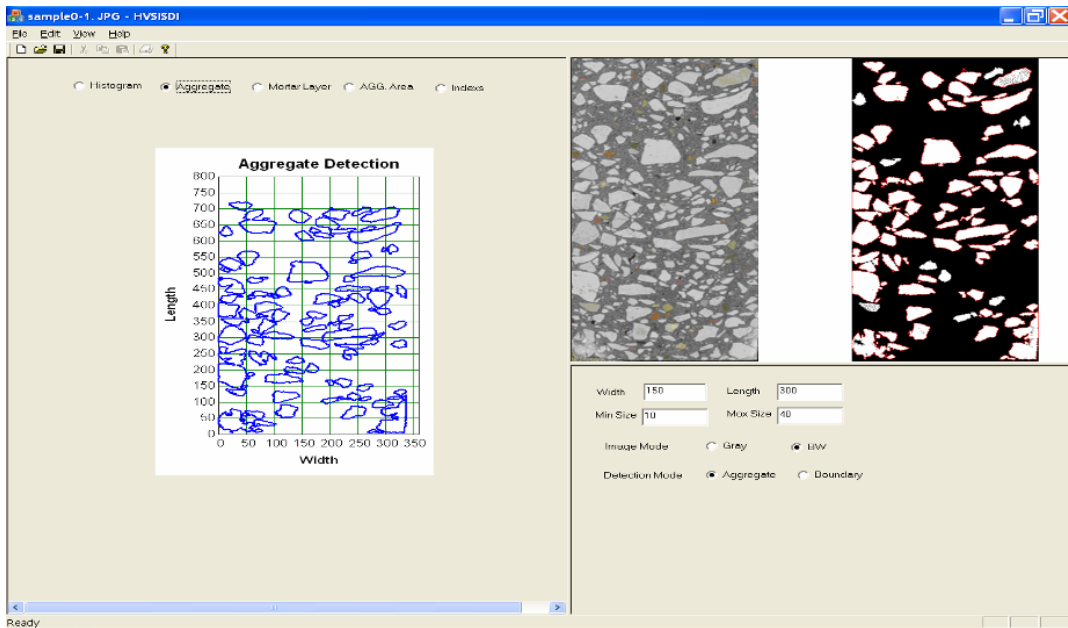


FIGURE 7 Evaluation System Software Interface.

FIGURE 8 shows the original image of a sample concrete cylinder. The figure also shows other images processed (using the algorithms developed in this paper) from the original sample on the basis of different aggregate sizing criteria. FIGURE 9 shows a screenshot showing the results of the statistical tests of aggregate size variance, length of the mortar layer, and the determined rating index (HVSI values).

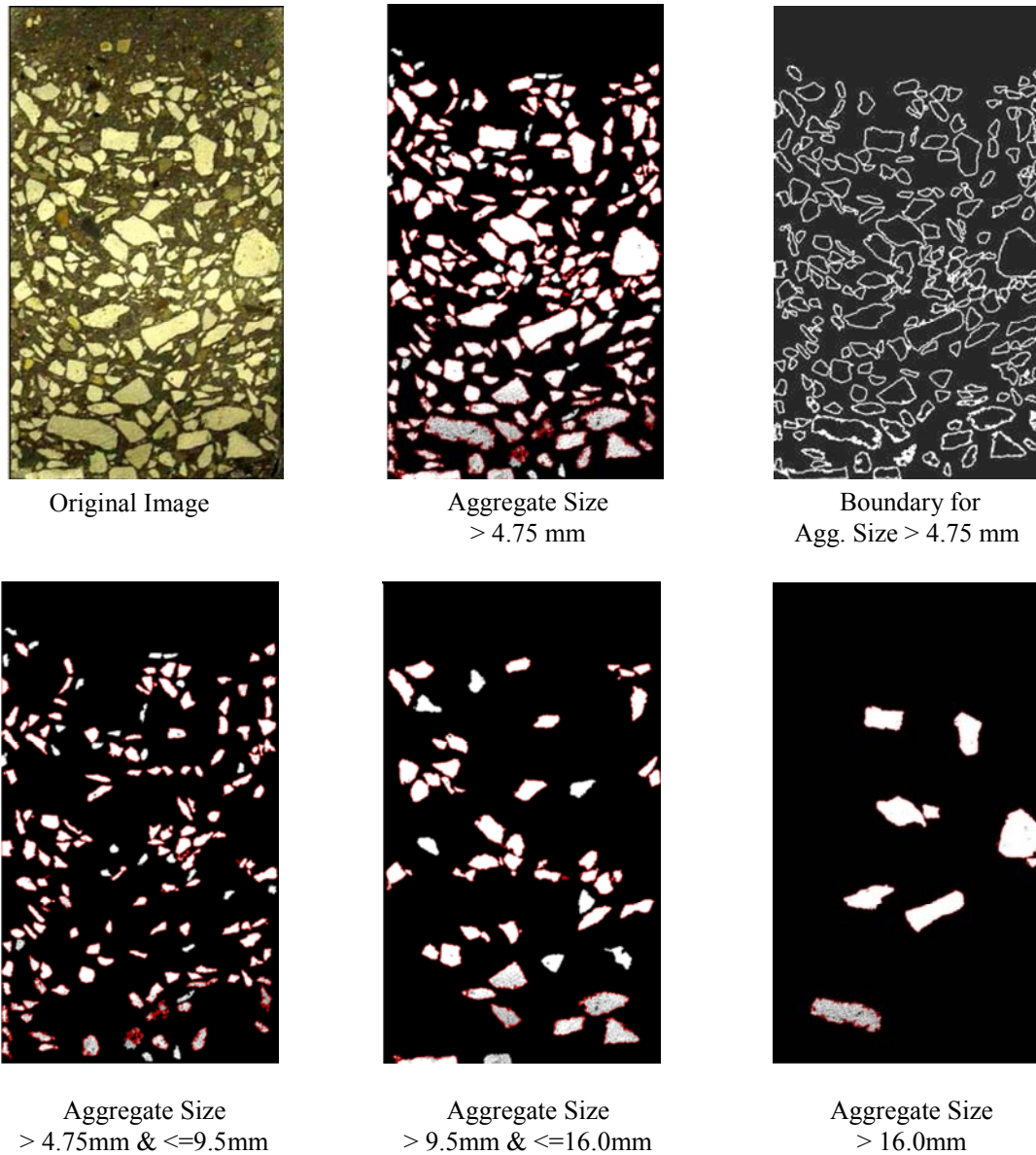


FIGURE 8 Processed Image of Sample Showing Various Aggregate Size Ranges.

Agg. Size Range	Section #	Section Position	5mm-Area Mean	5mm-Area Std. Dev.	T-Test t	P-Value	Index
From:4.75 To:9.50	1		89.64	36.47	1-2: 1.289	0.1052	1*0.0 = 0.0
	2		73.23	35.52	2-3: -1.612	0.0610	1*0.0 = 0.0
	3		94.77	39.93	1-3: -0.380	0.356	1*0.0 = 0.0
From:9.50 To:16.00	1		120.63	43.20	1-2: 1.871	0.0374	2*1.0 = 2.0
	2		85.51	61.43	2-3: 0.934	0.1900	2*0.0 = 0.0
	3		69.24	32.87	1-3: 3.786	0.000	2*2.0 = 4.0
From:16.00 To:100.00	1		43.79	52.10	1-2: -4.536	0.0000	4*2.0 = 8.0
	2		137.14	63.73	2-3: 3.630	0.0006	4*2.0 = 8.0
	3		63.72	49.84	1-3: -1.106	0.149	4*0.0 = 0.0
Summary	Total Index						22.0
	% Index						52.4
	Level of Variance in Size and Area						MID
	Mortar Length		Variance Level		Rating Index		
	34.0		MID		3-Unstable		

FIGURE 9 Screenshot Showing Sample Statistical Analyses and HVSI Determination.

VALIDATION OF THE DEVELOPED SYSTEM

The automated system for detection of aggregates and mortar layer and subsequently for HVSI measurement was tested for accuracy using 33 SCC cylinder images. The HVSI of these images were rated by a panel of experts, and then the developed system was used to determine the HVSI. TABLE 4 compares both HVSI measurements. The student T test for paired samples was carried out to ascertain whether there was any significant difference in results from the two measurement methods. The results (TABLE 5) showed that there is no significant difference in the results from these two test methods. This suggests that the HVSI measurements from the developed system are satisfactory.

TABLE 4 Validation of the Automated HVSI Assessment Tool

Sample ID	HVSI from Experts' Assessments	HVSI from Developed Tool	HVSI Deviation
1	2	2	0
2	1	2	1
3	2	3	1
4	0	0	0
5	0	0	0
6	1	1	0
7	1	2	1
8	1	0	-1
9	1	0	-1
10	1	1	0
11	1	1	0
12	3	3	0
13	3	3	0
14	3	3	0
15	0	0	0
16	2	2	0
17	1	0	-1
18	0	0	0
19	1	1	0
20	0	0	0
21	0	0	0
22	2	3	1
23	1	1	0
24	3	3	0
25	0	1	1
26	1	1	0
27	1	0	-1
28	2	2	0
29	2	2	0
30	2	2	0
31	3	3	0
32	3	3	0
33	0	0	0

TABLE 5 Pairwise T-Test Results

Test Method	HVSI from Experts' Assessments	HVSI from Developed System
Mean	1.33	1.36
Variance	1.104	1.426
Observation	33	33
Hypothesized Mean Difference	0	
Degrees of Freedom	32	
t	-0.328	
P ($T \leq t$) two-tail	0.744	
T Critical two-tail ($\alpha = 0.05$)	2.037	

SUMMARY AND CONCLUSIONS

This paper documented the development and implementation of algorithms for automatically measuring the static segregation resistance (stability) of SCC. The stability was measured in terms of a Hardened Visual Stability Index (HVSI). The automated system can replace the traditional (visual) assessment method as it overcomes the limitations of the latter such as human error, low efficiency, and work tedium. The automated process involves: digital processing of a concrete sample image, generation of a binary image of light colors (aggregates) and dark colors (concrete cement), identifying aggregate sizes and positions, detecting the mortar layer position and thickness, and assessing the concrete sample stability in terms of HVSI. The developed algorithms were implemented using standard coding languages. The accuracy of the automated system was checked using control observations and it was found that the new system is capable of reliably and consistently assessing concrete stability in terms of static segregation resistance. Notwithstanding the validation efforts of this paper, the conduction of further field tests is needed to completely validate the reliability of the algorithms.

The impetus for developing automated systems for construction quality assurance is rooted in emerging trends in the construction and transportation sectors. As more and more States turn to performance-based contracting and other innovative practices of construction delivery, there is an increasing need for quick, inexpensive, and reliable inspection of finished products. This need is particularly felt at the current time that is characterized by general trends in the current transportation environment such as uncertainty of sustained funding, increasing user expectations for shorter-period workzones, incipient retirement of the baby boomer generation and loss of its vast knowledge base, and general shortage of skilled engineering and inspection personnel. Opportunities for addressing this problem include the use of technology including image recognition. This paper exploits existing knowledge to address specific quality evaluation of a new type of high performance concrete.

Future Work

Possible enhancements to the developed system include color segmentation to replace or complement binary segmentation. This would improve the level to which aggregates of all colors (even dark shades) could be identified. Secondly, an additional algorithm could be developed to prevent the situation where separate multiple connected aggregates are mis-identified as larger aggregates. In the present study, the boundary tracking procedure is used solely for visualizing the aggregate size distributions. Possible future enhancements in this regard include improvement of aggregate detection by helping to discern whether a detected white area is only a single large aggregate or whether it actually consists of multiple small aggregates. It is expected that this enhancement would greatly minimize errors in aggregate recognition. Thirdly, future work could adapt the developed procedure to carry out an analysis of particle size distribution (gradation analysis) of cut surfaces of concrete made of ordinary Portland cement or asphaltic cement. Such cut surfaces may be cast concrete moulds or cored samples from hardened cast or cast concrete. Finally, the issue of image background can be addressed in future work. In the present study, the requirement for the input image is that it must contain only the image of the cut surface and no background of other material. In future, an enhanced system could overcome this limitation by automatically recognizing and distinguishing the concrete surface image from any other image and excluding the latter from the analysis.

ACKNOWLEDGMENTS

The authors acknowledge the critical support and guidance from James Krstulovich, concrete engineer at the Illinois Department of Transportation (IDOT), Gregg Larson, senior engineer at Applied Research Associates (ARA) and William Vavrik, division manager at ARA. Also, the authors wish to thank Xiaotian Wang and Les Rabe of ARA for their contributions. The contents of this paper reflect the views of the authors, who are responsible for the facts and the accuracy of the data presented herein, and do not necessarily reflect the official views or policies of IDOT or ARA.

REFERENCES

1. Khayat, K.H. Workability, Testing, and Performance of Self-Consolidating Concrete, *ACI Materials Journal*, Nr. 96-M43. pp. 346-354, 1999.
2. *The European Guidelines for Self-Compacting Concrete Specification, Production and Use*, Self Compacting Concrete European Project Group, May 2005.
3. Ouchi, M., Nakamura, S., Osterberg, T., Hallberg, S., and Lwin, M. Applications of Self-Compacting Concrete in Japan, Europe and the United States, *Proceedings of the 5th International Symposium on High Performance Computing*, Eds: Veidenbaum, A., Kazuki, J., Amano, H, Aiso, H. October 20-22, 2003, Tokyo-Odaiba, Japan.
4. *Concrete in Practice, Where, How, Why, CIP 37 Self Consolidation Concrete (SCC)*, National Ready Mix Concrete Association, Silver Springs, MD, 2005.
5. *ASTM C143, Annual Book of ASTM Standards, Volume 04.02 Concrete and Aggregates*, American Society for Testing and Materials, 2000.
6. Concrete Technology – Frequently-asked Questions. Portland Cement Association http://www.cement.org/tech/faq_scc.asp. Accessed April 12, 2006.
7. *Standard Test Method for Static Segregation of Hardened Self-Consolidating Concrete Cylinders, Illinois Test Procedure SCC-6*. Illinois Department of Transportation, Peoria, IL, 2005
8. Davies, E. R. *Machine Vision: Theory, Algorithms, Practicalities, 3rd Edition*, Morgan Kaufmann Publishers, San Francisco, CA, 2004.
9. Imagemagick. <http://www.imagemagick.com>. Accessed April 12, 2005.
10. Cormen, T. H., Leiserson, C. E., and Rivest, R. L. *Introduction to Algorithms*, MIT Press, Cambridge, Massachusetts, London, England, 1997.